Energy-Optimal Kinodynamic Planning for Underwater Gliders in Flow Fields

James Ju Heon Lee[1], Chanyeol Yoo[1], Raewyn Hall[2], Stuart Anstee[2] and Robert Fitch[1]
[1]Centre for Autonomous Systems, University of Technology Sydney, NSW Australia
juheon.lee@student.uts.edu.au, {chanyeol.yoo, robert.fitch}@uts.edu.au
[2]Defence Science and Technology Group, Department of Defence
{raewyn.hall, stuart.anstee}@dst.defence.gov.au

Abstract

We consider energy-optimal navigation planning in flow fields, which is a long-standing optimisation problem with no known analytical solution. Using the motivating example of an underwater glider subject to ocean currents, we present an asymptotically optimal planning framework that considers realistic vehicle dynamics and provably returns an optimal solution in the limit. One key idea that we introduce is to reformulate the dynamic control problem as a kinematic problem with *trim states*, which encapsulate the dynamics over suitably long distances. We report simulation examples that, surprisingly, contravene the use of regular 'sawtooth' paths currently in widespread use. We show that, when internal control mechanics are taken into account, energy-efficient paths do not necessarily follow a regular up-and-down pattern. Our work represents a principled planning framework for underwater gliders that will enable improved navigation capability for both commercial and defence applications.

1 Introduction

Many outdoor vehicles are subject to external disturbances that can be modelled as flow fields. Examples include commercial aircraft travelling through wind in a fuel-efficient manner [Yoo *et al.*, 2014; Girardet *et al.*, 2014; M. *et al.*, 2015], aerial gliders exploiting thermal airflows [Yoo *et al.*, 2012; Cobano *et al.*, 2013; Nguyen *et al.*, 2013], and underwater gliders that persistently monitor large areas subject to ocean currents [Fernndez-Perdomo *et al.*, 2010; Isern-Gonzalez *et al.*, 2011; Tesei *et al.*, 2015]. These outdoor platforms are typically difficult to refuel or recharge while in operation; we are interested in energy-efficient planning that exploits existing flow fields to achieve maximum mission duration. This long-standing optimisation problem has remained open for nearly a century and, unfortunately, still has no known analytical solution [Zermelo, 1931].

Another complicating factor is that such outdoor vehicles often have complex dynamics [Zarafshan *et al.*, 2008; Mahmoudian *et al.*, 2010; Lawrance and Sukkarieh, 2011]. Their dynamical models are typically non-linear and the control space is too large to find a feasible solution in a timely manner. For instance, a *SLOCUM*-type underwater glider [Leonard and Graver, 2001; Jones *et al.*, 2014] is controlled by physically moving control masses inside the vehicle and pumping in or out water from the ballast tank. Because the energy expenditure of such a glider is directly affected by the control inputs, a coarse representation may call into question the integrity of any control solution found.

Our motivating example is long-duration navigation for underwater gliders under the influence of ocean currents. We would like to efficiently control the glider through ocean currents, avoid obstacles, and reach a given destination while minimising energy expenditure. This problem has been addressed using oversimplified kinematic and energy models with poor computational efficiency and limited or no performance guarantees [Lolla *et al.*, 2014b; 2014a].

In this paper, we present an asymptotically optimal planning framework for underwater gliders with realistic dynamics. The glider operates in the ocean with time-invariant current flows that the glider may avoid or exploit to save energy while avoiding obstacles. Unlike most previous approaches to this problem, which assume direct controllability of glider pose, we instead assume an unrestrictive dynamic model where pose is controlled implicitly through internal hydraulics. We reduce a high-dimensional dynamic model of the glider to a more parsimonious 6-dimensional kinematic model by considering a *trim state*: the state of dynamic equilibrium in which the glider continues indefinitely in a straight line in the absence of active controls. We consider a path expressed as a sequence of glider kinematic

states where a trim state exists between any consecutive kinematic states. Given the kinematic model, we find the energy-optimal path between the initial and goal states by adapting a sampling-based planning algorithm called *fast marching tree** (FMT*) [Janson *et al.*, 2015] which guarantees asymptotic optimality and converges quickly in high-dimensional configuration spaces compared to traditional algorithms such as RRT* and PRM* [Frazzoli and Karaman, 2011]. We argue that our adaptation to FMT* retains its original performance guarantees.

We validate the proposed framework using complicated flow fields and obstacles, including different types of vortices and seabed topographies. Our results exhibit interesting counter-intuitive paths which we discuss extensively. In particular, we show that the classical periodic 'sawtooth'-shaped manoeuvre in depth is not always energy efficient. We compare our result with current state-of-the-art algorithms [Kularatne *et al.*, 2016] and discuss the difference and significance of our framework in terms of the state space and depth profile.

The significance of this work is primarily to improve the navigation capability of underwater gliders through energy-efficient paths. Although the presentation of our method is specific to underwater gliders, the design principles could be useful for application to other types of vehicles.

This paper is organised as follows. In Sec. 2 we briefly discuss related work. In Sec. 3, we formally state the problem and define models of the glider and the ocean current. In Sec. 4, we formally define and compute the glider's trim state, and in Sec. 5, we present an asymptotically optimal planning algorithm. We demonstrate simulated examples using different environment settings in Sec. 6 and conclude the paper in Sec. 7.

2 Related Work

Various approaches have been presented to solve path planning problems for autonomous surface and underwater vehicles (ASVs and AUVs) in flow fields [Kularatne *et al.*, 2016; Fernndez-Perdomo *et al.*, 2010; Xinke *et al.*, 2015; Isern-Gonzalez *et al.*, 2011]. Often the dynamics of the vehicles are given as a classical 2-dimensional kinematic model where the turning rate is directly controlled. Based on the simple model, the objective is to minimise the time and energy. In most of the cases, energy use is modelled simply as a linear function of time; optimal solutions are often achieved by maximising the resultant velocity against the currents.

There also exists work that considers manoeuvres of underwater gliders in 3-dimensional space [Liu *et al.*, 2017; Cao *et al.*, 2017]. However, this work also uses a simple kinematic model with directly controllable turning rates. Based on the vehicle model in [Cao *et al.*, 2017], a Dubins path is given as an optimal solution consisting of a series of 'sawtooth' and spiral motions. In our paper, we prove by examples and discussions that such manoeuvres are unlikely to be optimal with respect to the more accurate glider model we introduce.

Existing approaches also generally oversimplify the complex dynamics of the vehicles. For example, the *SLOCUM*-type underwater gliders [Leonard and Graver, 2001] may be accurately modelled as a system of nonlinear equations over high-dimensional state space. Such a glider is controlled by moving masses and pumping water in and out of its ballast tank. Since energy consumption is based on the mechanics/hydraulics of this control system, a simple energy cost model may be misleading and could cause failure at the limit of the glider's energy capacity. Therefore, accurately modelling the glider dynamics in planning is mandatory. In our paper, we present a glider model that is both computationally efficient and representative of the real dynamics.

A number of planning algorithms have been used to solve similar path planning problems in flow fields. Graph-based algorithms including A* [Kularatne *et al.*, 2016; Fernndez-Perdomo *et al.*, 2010; Isern-Gonzalez *et al.*, 2011] and sampling-based algorithms such as RRT [Ko *et al.*, 2014] have been widely used. In [Rao and Williams, 2009], both A* [Witt and Dunbabin, 2014] and RRT are applied, but these algorithms cannot offer analytical performance guarantees.

Recently, FMT* was presented as a novel sampling-based motion planning algorithm [Janson *et al.*, 2015] that guarantees asymptotic optimality. Based on the PRM* and RRT* algorithms [Frazzoli and Karaman, 2011], FMT* uses lazy collision checking to reduce the inherent bottleneck in sampling-based algorithms, and it is shown to converge much faster in high-dimensional problems than its predecessors. In this paper, we adapt FMT* for our purposes while preserving its important analytical properties.

3 Problem Formulation

Suppose we have an underwater glider, described by a 12-dimensional dynamical model

$$\dot{\mathbf{x}}(t) = f(\mathbf{x}(t), \mathbf{u}(t)) + \mathbf{V}_c(t), \tag{1}$$

where $\mathbf{x}(t)$ is the glider state at time t, $\mathbf{u}(t)$ is the control vector, and $\mathbf{V}_c$ is the flow velocity vector. Figure 1 shows an approximate representation of the forces and moments acting on the inertial reference frame of the glider. More details can be found in [Leonard and Graver, 2001]. The control vector $\mathbf{u}(t) = [\mathbf{u}_{\mathbf{r}_p}(t), \mathbf{u}_{m_b}(t)]^T$ consists of forces acting on the moving mass $\mathbf{u}_{\mathbf{r}_p} = \dot{P}_{\mathbf{r}_p}$ where $\mathbf{r}_p = [x_p, y_p, z_p]^T$ and the rate of changing ballast mass $\mathbf{u}_{m_b} = \dot{m}_b$. Note that the ballast mass is changed by pumping in or out water into the ballast tank.

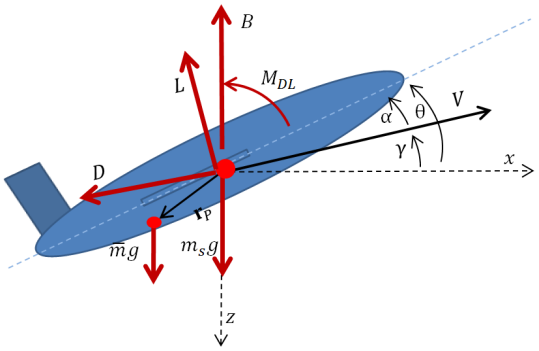

Figure 1: An approximate representation of the forces and moments acting on the glider in the inertial reference frame. The hydrostatic forces consists of the buoyancy force B, weight due to moving mass $\bar{m}g$, weight due to stationary mass m_sg; the hydrodynamic forces consists of lift L, drag D and the pitching moment M_{DL}. The moving mass offset from the nominal centre of gravity by a vector r_p The glide angle γ, pitch angle θ and angle of attack α represent the orientation and direction of the glider with velocity V

The discrete-time dynamical model of the glider is

$$\mathbf{x}[k+1] = F(\mathbf{x}[k], \mathbf{u}[t]) + \mathbf{V}_c[t]. \tag{2}$$

Given the discrete model and a sequence of control vectors $\mathbf{U}[k] = \{\mathbf{u}[0], \mathbf{u}[1], \cdots, \mathbf{u}[k]\}$, the sequence of glider state vector is recursively found as $\mathbf{X}[k+1] = \{\mathbf{x}[0], \mathbf{x}[1], \cdots, \mathbf{x}[k+1]\}$.

The time-invariant velocity vector of the ocean current at a given position vector $\mathbf{p} = [x, y, z]^T$ is given *a priori*, such that

$$\mathbf{V}_c(t) = \begin{bmatrix} u_c & v_c & w_c \end{bmatrix}^T, \tag{3}$$

where $\mathbf{V}_c$ is a velocity vector in xyz-directions.

The glider's energy expenditure comes from the control of the glider (i.e., forces acting on the masses) and the *hotel load* (e.g., onboard processor and sensors). Given a state $\mathbf{x}[k]$ and a control $\mathbf{u}[k]$, the glider's energy cost is denoted as $cost(\mathbf{x}[k], \mathbf{u}[k])$. The energy cost for a sequence of control vectors is given as $cost(\mathbf{x}[k], \mathbf{U}[k : k+n])$

We consider the following planning problem with the glider in a flow field:

Problem (Energy-optimal path planning for underwater glider)**.** *Given an initial state* $\mathbf{x}[0] = \mathbf{x}_{init}$ *and a set of goal states* $\mathbf{X}_g$*, find an energy-optimal fnite sequence of control vectors* $\mathbf{U}^*$*, such that*

$$\begin{aligned} \mathbf{U}^* = & \underset{\mathbf{U}=\{\mathbf{u}[0],\cdots\}}{\arg\min} \quad \mathrm{cost}(\mathbf{x}[0], \mathbf{U}) \\ & s.t.\ \mathbf{x}[last] \in \mathbf{X}_g. \end{aligned} \tag{4}$$

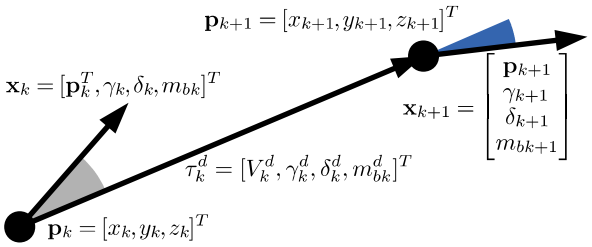

(a) Transition from state $\mathbf{x}_k$ to $\mathbf{x}_{k+1}$. A desired trim condition τ_k^d is found between $\mathbf{p}_k$ and $\mathbf{p}_{k+1}$

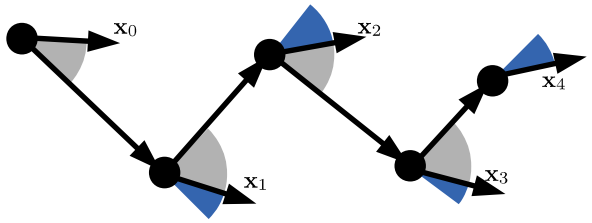

(b) Sequence of state vectors and trim states

Figure 2: Kinematic model for 6D glider. Gray shade represents initial control from initial glider state to trim state, and the blue represents the control from trim state to final glider state.

By executing a sequence of control inputs $\mathbf{U}^*$ from the initial state $\mathbf{x}[0]$, we get the energy-optimal path $\mathbf{X}^*$ that leads to one of the goal states $\mathbf{X}_g$.

4 Gliding Trim State

Assuming the glider operates over long distances, we can reformulate the dynamic control problem to be more computationally convenient. A *trim state* is a state of dynamic equilibrium in which a vehicle will continue indefinitely in the absence of disturbances or variations to control inputs [Leonard and Graver, 2001]. Because the glider covers a significantly large area over time and a small amount of energy is required in the absence of control, we assume that the glider would operate in a series of trim states with negligible control time between the states. With this property, we reduce the dynamic problem into a kinematic problem where the glider's kinematic state vector consists of 6 variables, such that

$$\mathbf{x}_k = \begin{bmatrix} x_k & y_k & z_k & \gamma_k & \delta_k & m_{bk} \end{bmatrix}^T, \tag{5}$$

where (x, y, z) is the position, γ is the glide angle, δ is the heading angle, and m_b is the ballast mass (i.e., amount of water in the ballast tank). We assume that the ballast tank is either empty or full (i.e., $m_b \in [0, m_{b\,\max}]$).

Suppose we have a sequence of state vectors $\mathbf{X}_k = \{\mathbf{x}_0, \mathbf{x}_1, \cdots, \mathbf{x}_k\}$ and the corresponding position vectors $\mathbf{P}_k = \{\mathbf{p}_0, \mathbf{p}_1, \cdots, \mathbf{p}_k\}$, where $\mathbf{p}_i = [x_i, y_i, z_i]^T$. An example of such a sequence is shown in Fig. 2b. We consider a trim state $\boldsymbol{\tau}_k^d$ between two position vectors $\mathbf{p}_k$

and $\mathbf{p}_{k+1}$, such that

$$\boldsymbol{\tau}_k^d = \begin{bmatrix} V_k^d & \gamma_k^d & \delta_k^d & m_{bk}^d \end{bmatrix}^T, \tag{6}$$

as shown in Fig. 2a. Note that d stands for *desired*.

With the trim state-based manoeuvre, we approximate the dynamical path planning problem and re-define the problem as follows:

Problem (trim state-based path planning)**.** *Given initial and goal states, find an energy-optimal series of state vectors* $\mathbf{X}^*$*, such that a valid trim state* $\boldsymbol{\tau}_k^d$ *between state vectors* $\mathbf{x}_k$ *and* $\mathbf{x}_{k+1}$ *is found.*

The optimal states $\mathbf{X}^*$ could be considered as a series of waypoints to follow. In this formulation, the variations to control inputs are made in two cases: 1) from the initial kinematic state $\mathbf{x}_k$ to the trim state $\boldsymbol{\tau}_k^d$, and 2) from trim state to the next state $\mathbf{x}_{k+1}$. We assume that the state transitions between a kinematic state and a trim state is instantaneous, because the state transition time is negligible compared to the gliding time in a trim state.

4.1 Computing a trim state

Within a trim state, the glider is moving in a straight line, described as

$$\mathbf{p}_{k+1} = \mathbf{p}_k + \left(\begin{bmatrix} V_k(\gamma)\cos\gamma\cos\delta \\ V_k(\gamma)\cos\gamma\sin\delta \\ V_k(\gamma)\sin\gamma \end{bmatrix} + \begin{bmatrix} u_c \\ v_c \\ w_c \end{bmatrix} \right) \Delta t, \tag{7}$$

where the flow vector is the average between the initial and final position vectors $\mathbf{p}_k$ and $\mathbf{p}_{k+1}$. We rearrange the z-term from (7) to get

$$\Delta t = \frac{z_f}{V_k(\gamma)\sin\gamma + w_c}. \tag{8}$$

We substitute Δt to the x- and y-th terms and rearrange them into the form $\sin^2\delta + \cos^2\delta = 1$:

$$\begin{aligned} &\left(\frac{x_f}{z_f}(V_k \sin\gamma_d + w_c) - u_c \right)^2 \\ &+ \left(\frac{y_f}{z_f}(V_k \sin\gamma_d + w_c) - v_c \right)^2 \end{aligned} = {V_k}^2 \cos^2\gamma_d. \tag{9}$$

We find the desired trim condition $\boldsymbol{\tau}_d$ by numerically solving the non-linear equation above. In this paper, we sample a set of evenly spaced glide angles Γ_d and enumerate the values in the set to find the solution satisfying the equation in (9) by finding

$$(\gamma^*, m_b^*) = \underset{\gamma\in\Gamma_d, m_b\in[0, m_{b\,\max}]}{\arg\min} \|\mathrm{LHS}(\gamma, m_b) - \mathrm{RHS}(\gamma, m_b)\|, \tag{10}$$

where LHS and RHS are the left and right hand side of (9). Note that V_k is the function of γ and m_b, and the heading angle δ_k can be derived from (7) using γ^*.

Since the trim velocity V_k is a function of glide angle γ and ballast mass m_b, and the heading angle δ is an independent variable, we only need the glide angle γ that satisfies the equation for a given position change $\mathbf{p}_{k+1} - \mathbf{p}_k = (x_f, y_f, z_f)$ and the current vector. Because the terms $(V_k \sin\gamma)$ and $(V_k \cos\gamma)$ are invariant with position change, we could pre-calculate once at the start of the framework, and use them for the rest of the computations.

The set of glide angles Γ_d is restricted to be sampled as follows

$$\Gamma_d \subset \left[\tan^{-1}\left(\frac{-2K_{D_0}}{K_{L_0} \mp \sqrt{K_{L_0}^2 + K_{L_0} J_L^2 / K_D}} \right), \pm 60^\circ \right], \tag{11}$$

where the maximum glide angle is heuristically chosen for safety. It is important to note that the minimum glide angle is limited by the glider dynamics.

For a given trim state $\boldsymbol{\tau}_k^d$, we find the corresponding control vector $\mathbf{u}$. More details on the kinematic state variables can be found in Appendix A.

4.2 Energy cost

The total energy consumption E_{total} is given as a sum

$$\mathrm{E}_{total} = \mathrm{E}_{\Delta B} + \mathrm{E}_H + \mathrm{E}_{\Delta x_p} + \mathrm{E}_{\Delta\delta}, \tag{12}$$

where 1) $\mathrm{E}_{\Delta B} = -\eta_p g z \Delta m_b$ is the energy required to empty the ballast tank, which depends on the static pressure (i.e., depth from surface), 2) $\mathrm{E}_{\Delta x_p} = \eta_m \cdot \bar{m} \cdot \Delta x_p$ is the energy required to change the gliding angle λ by changing the position of the moving mass x_p, 3) $\mathrm{E}_{\Delta\delta} = \eta_\delta \cdot \Delta\delta$ is the energy required to change the heading angle, and 4) $\mathrm{E}_H = L_H \cdot \Delta t$ is the hotel cost. It is important to note that the energy consumption based on our model depends on the internal non-linear dynamics, as opposed to other existing work where energy model is over-simplified.

Given two vehicle states $\mathbf{x}_k$ and $\mathbf{x}_{k+1}$, the energy cost is the sum of the following processes: 1) from state $\mathbf{x}_k$ to trim state $\boldsymbol{\tau}_k^d$, 2) during trim state $\boldsymbol{\tau}_k^d$, and 3) from trim state $\boldsymbol{\tau}_k^d$ to state $\mathbf{x}_{k+1}$. Note that the hotel cost only exists during the trim state because we assume that the time it takes for trim state transition is negligible compared to the manoeuvre. In this paper, the cost for a sequence of state vectors $\mathbf{X}$ is expressed as $cost(\mathbf{X})$, and that for a transition between two state vectors is $cost(\mathbf{x}, \mathbf{y})$.

5 Asymptotically Optimal Planning

In this section, we present our implementation of FMT*. We highlight variations made to the algorithm to be applicable to the underwater glider case.

Algorithm 1 Abridged FMT* Algorithm

$V \leftarrow \{x_{init}, x_{goal}\} \cup SampleFree(n)$
$V_{unvisited} \leftarrow V \setminus \{x_{init}\}; V_{open} \leftarrow \{x_{init}\}; V_{closed} \leftarrow \emptyset$
while Solution not found **do**
  $z \leftarrow min\{c(V_{open})\}$
  $xNear \leftarrow neighbour(z, V) \cap V_{unvisited}$
  for all $x \in xNear$ **do**
    $yNear \leftarrow neighbour(x, V) \cap V_{open}$
    $y_{min} \leftarrow arg\, min_{y \in yNear}\{c(y) + Cost(y, x)\}$
    if $noCollision(y_{min}, x)$ **then**
      $addEdge(y_{min}, x)$
    end if
  end for
  move all connected x from $V_{unvisited}$ to V_{open}
  $V_{open} \leftarrow V_{open} \setminus \{z\}; V_{closed} \leftarrow z$
  if $V_{open} = \emptyset$ **then**
    return Failure
  end if
end while
return Sequence of waypoints

Like PRM*, the FMT* algorithm starts with a set of sample points in the state space. In this paper, we sample states $\mathbf{V}$ over the 6-dimensional kinematic state space. Note that each sampled state $v \in V$ is a trim state $[x, y, z, \gamma, \delta, m_b]^T$. Instead of randomly sampling the states across the dimensions, we first choose N_p samples over the position space (x, y, z), and then uniformly sample N_a angle states (γ, δ) for each position state. Because we assume the ballast tank is either empty or full (i.e., $m_b \in \{0, m_{b\,\max}\}$), the overall number of samples is $N_s = N_p \cdot N_a \cdot 2$. The sampled states are initially labelled as *unvisited* except the starting position $\mathbf{x}_0$ which is labelled as *opened*.

The algorithm incrementally grows a branching tree that eventually finds an optimal solution. At a given instance, we first find an open state z with the lowest overall cost. From z, we find a set of unvisited states $xNear$ that incur the least transition cost. For each unvisited state $x \in xNear$, we find the open state y such that the sum of the cost at y and the transition cost from y to x is the minimum. After we find such an open state y, we then check if the transition is collision free. If so, we set z to *closed* and any newly connected states in $xNear$ become *opened*. We continue growing the tree until we reach the goal state or when no more *open* states exist. Pseudocode is presented in Alg. 1.

5.1 Analysis

Finding the nearest neighbours, the most time consuming task in sampling-based planners, is handled efficiently by the concept of *mutual connectivity*. FMT* assumes that if state x is one of the N-nearest neighbours of state y, then state y is also one of the N-nearest neighbours of state x. This is important because it eliminates duplicate computations in finding the nearest neighbours when we find $xNear$ from z and y from $x \in xNear$. More formally, mutual connectivity assumes $cost(a, b) \equiv cost(b, a)$ In this paper, the mutual connectivity may not hold true because of the dynamical constraints (i.e., $cost(a, b) \not\equiv cost(b, a)$). However, we slightly abuse the definition so that the cost function $cost^*$ in our implementation is forced to be directional. Formally speaking,

$$cost^*(a, b) = \begin{cases} cost(a, b) & \text{if } a \text{ is opened and } b \text{ is unvisited} \\ cost(b, a) & \text{otherwise} \end{cases}. \tag{13}$$

With the directional cost function, we always guarantee that the cost is computed from open to unvisited states. As a consequence, our implementation holds true for mutual connectivity and asymptotic optimality is preserved.

We also exploit the important property of FMT* called 'lazy' collision checking, where the collision between two states is checked after a candidate transition is computed. This crucial property of FMT* improves the computation time significantly, because collision checking is usually the most time consuming operation in sampling-based planning methods.

6 Case Studies

In this section, we demonstrate simulated examples for different flow fields and obstacle types. The combinations of the flow fields and obstacles are chosen to demonstrate how the framework finds an energy-optimal path by using the flow fields. We show counter-intuitive solutions and discuss them in terms of the interesting mechanics of the glider. We also compare our approach with state-of-the-art work in the field and discuss why our approach is more realistic and valid.

The model of the underwater glider was described in Sec. 3 with parameters in Appendix B. Using the planning algorithm presented in Sec. 5, an optimal path with respect to energy cost, described in Sec. 4.2, is found. The framework is implemented using C++ within the standard planning library called *OMPL* [Şucan *et al.*, 2012]. The simulation is planned under a 6-Dimensional state space described in Sec. 4. The kinematic states are shown in SI units with angles in radians.

6.1 Opposing current

In this case study, we demonstrate a glider path from initial kinematic state $[50, 0, 5, -0.2, 0, 2]^T$ to $[950, 0, 5, 0.2, 0, 0]^T$. The glider has to traverse against an opposing current that linearly decays with

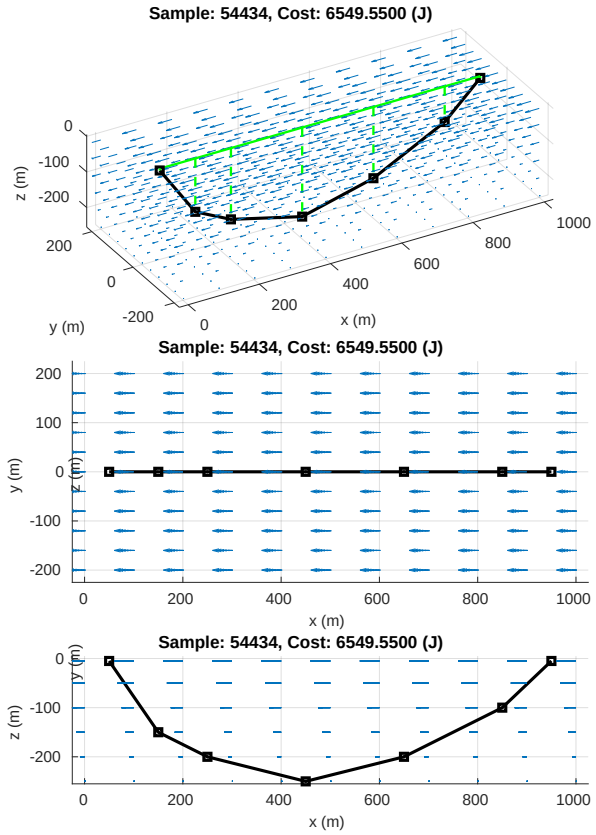

Figure 3: Opposing current with no obstacle

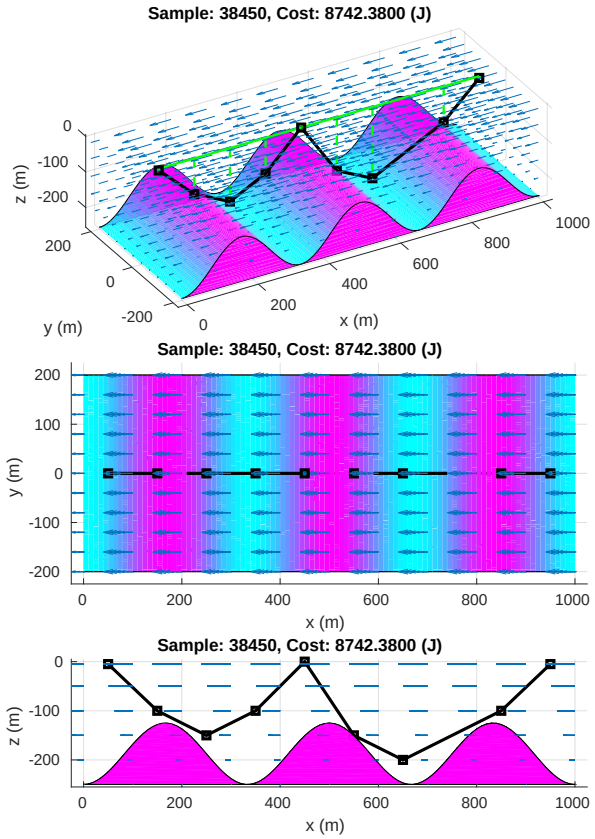

Figure 4: Opposing current with 3 sand dunes

depth as shown in Fig. 3 with 3D, top-down and side views.

The parabola-shaped depth profile is interesting compared to 'sawtooth'-shaped paths, which are often assumed to be efficient. Surprisingly, after we consider the depth profile and the energy consumption associated with changing the depth (i.e., changing the ballast mass m_b and pushing the movable mass $\bar{m}$), our path avoids such manoeuvres. Note that filling the ballast tank is assumed to be cost-free; diving down does not incur energy consumption. Also, there exists no further energy loss as long as the state of the tank does not change. As a consequence, the only instance of energy loss due to the ballast tank is at the bottom where we pump out water from the tank.

6.2 Opposing current with sand dunes

In this example, we consider a case where there exist sand dunes on the ocean floor, with the same initial and goal states and linearly decaying opposing current as in Sec. 6.1.

Although we have the same ocean current and states of interest, the behaviour of the glider is interestingly different to the previous example. In Sec. 6.1, we have shown that the energy-efficient path for the linearly decaying currents is a parabola-shaped curve in the absence of obstacles. However, in this example, we no longer can execute such control inputs due to collisions. In Fig. 4, we demonstrate the energy-efficient glider path avoiding collision. The glider initially dives down to avoid the strong opposing current and then goes up to avoid the sand dune.

Intuitively, the glider would have to follow the dune's curvature in order to avoid strong opposing currents. However, the energy-efficient path contradicts this intuition for the following reasons. First the glider does not dive too deep because it would have to empty the ballast tank twice. Note that the cost of emptying the ballast tank increases with the depth. Secondly, the strong opposing current near the surface forces a steep angle of ascent (e.g., around $x = 450$).

6.3 Quad vortices

We demonstrate an example with four rotational vortices, previously presented in [Kularatne *et al.*, 2016] for the case of surface vehicle (e.g., boat). Note that the examples from the work were over the xy-plane. We have extended an additional depth dimension for this case study. Figure 5 shows the energy-efficient glider path from $[0, 0, 5, -0.2, 0, 2]^T$

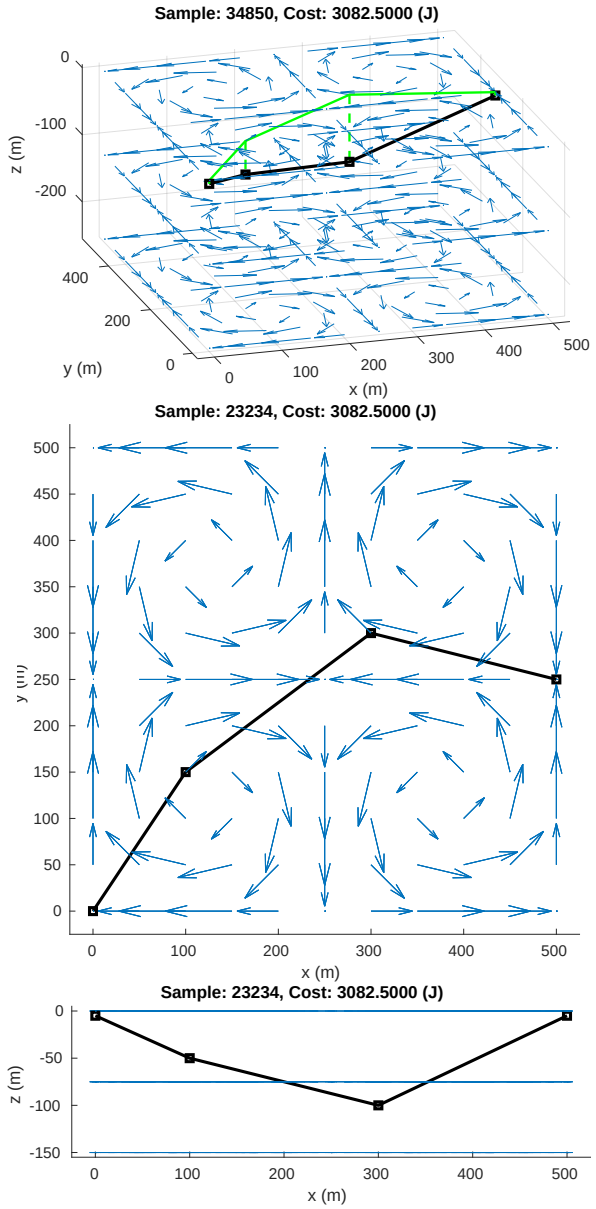

Figure 5: Quad vortices (test 1)

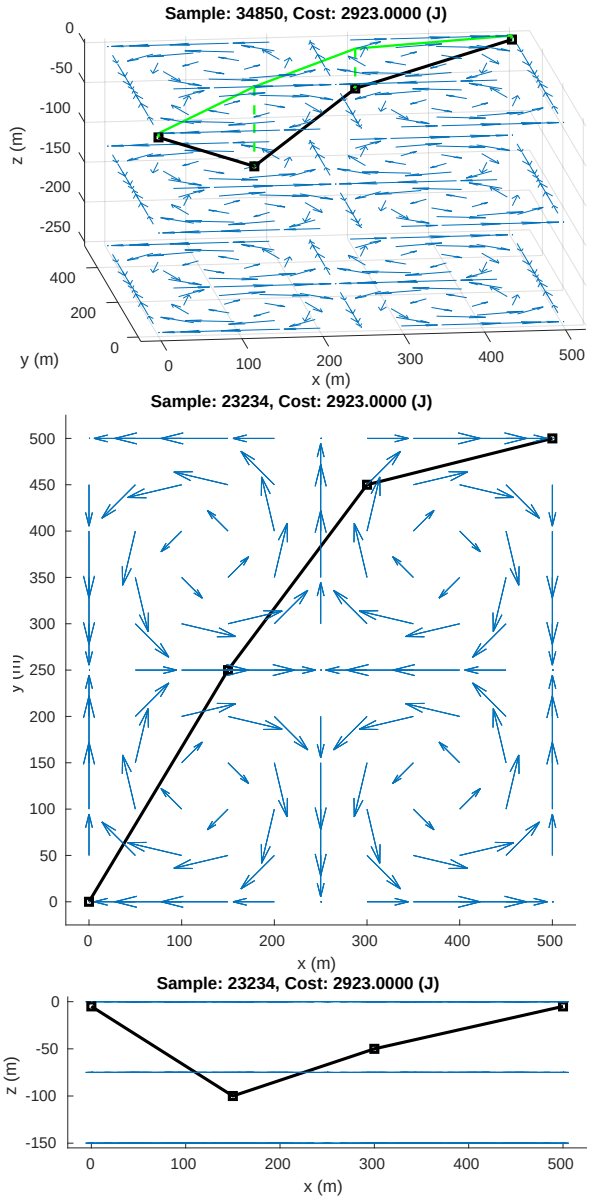

Figure 6: Quad vortices (test 2)

to $[500, 250, 5, 0.2, 0, 0]^T$, and Fig. 6 shows that from $[0, 0, 5, -0.2, 0, 2]^T$ to $[500, 500, 5, 0.2, 0, 0]^T$.

By introducing the depth profile for the glider, the shapes of our paths are counter-intuitive compared to other existing work. The paths in previous work tend to be more smoothly varying and move as close to the currents as possible. This is because there exists no energy loss due to depth changes. However, we have shown throughout this paper that the underwater glider consumes a significant amount of energy while changing its depth. As a consequence, our paths are coarser and generated from only a few waypoint states to follow. Again, we show that our solution considering the depth profile avoids the 'sawtooth'-shaped trajectories.

6.4 Irrotational flows with island

In this example, we consider an example with an island obstacle and two sources of irrotational currents as shown in Fig. 7 with 3D, top-down and side views. The glider initially starts from $[50, -100, 5, -0.2, 0, 2]^T$, and reaches its goal on $[950, 100, 5, 0.2, 0, 0]^T$.

Similar to the previous example, the path in this example is quite coarse and not as smoothly varying as those in other work. As already described, the manoeuvre in our solution avoids the significant energy loss which otherwise would be incurred by changing depth.

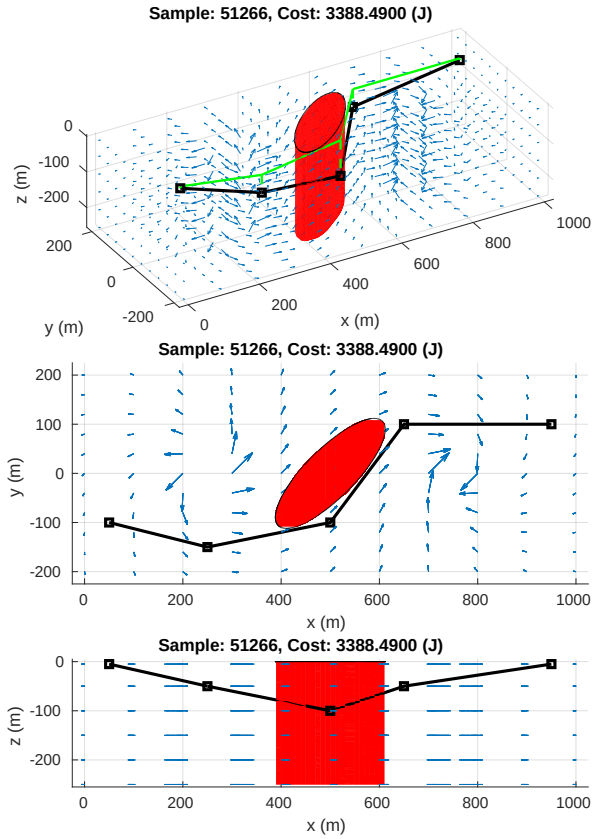

Figure 7: Island obstacle with two irrotational vortices

Note that there is only one instance of energy loss due to depth change (i.e., at the bottom) when the ballast tank is emptied. While considering the depth constraint, the glider exploits the current flows by gliding in the same direction, reducing the energy loss due to the hotel load (i.e., reducing the time spent).

7 Conclusion and Future Work

In this paper, we addressed the problem of path planning in the presence of flow fields for underwater gliders with complex dynamics. We introduced a trim state-based control approach by reformulating the complex dynamical model into a kinematic model with trim states. Based on the reduced control space, we have implemented the state-of-the-art sampling-based planning algorithm, FMT*, while preserving its important properties. The glider model is computationally efficient and the solution is realistic, which we demonstrate in a series of examples. We showed that the depth profile is significant in planning over flow fields, because the energy expenditure during a depth change is significant. The most important avenue of future work is to develop a probabilistic variant of the framework that would consider actuation and localisation uncertainty.

Acknowledgement

This work was funded by Defence Science and Technology Group under the Trusted Autonomy Strategic Research Initiative.

References

[Cao *et al.*, 2017] J. Cao, J. Cao, and Z. Zeng. Toward Optimal Rendezvous of Multiple Underwater Gliders: 3D Path Planning with Combined Sawtooth and Spiral Motion. *J. Intell. Robot. Syst.*, 85(1):189–206, 2017.

[Cobano *et al.*, 2013] J. A. Cobano, A. D., S. Sukkarieh, G. Heredia, and A. Ollero. Thermal detection and generation of collision-free trajectories for cooperative soaring UAVs. In *Proc. of IEEE/RSJ IROS*, pages 2948–2954, 2013.

[Fernndez-Perdomo *et al.*, 2010] E. Fernndez-Perdomo, J. Cabrera-Gmez, D. Hernndez-Sosa, J. Isern-Gonzlez, A. C. Domnguez-Brito, A. Redondo, J. Coca, A. G. Ramos, E. . Fanjul, and M. Garca. Path planning for gliders using Regional Ocean Models: Application of Pinzn path planner with the ESEOAT model and the RU27 trans-Atlantic flight data. In *Proc. of IEEE OCEANS*, pages 1–10, 2010.

[Frazzoli and Karaman, 2011] E. Frazzoli and S. Karaman. Sampling-based algorithms for optimal motion planning. *Int. J. Rob. Res.*, 30(7):846–894, 2011.

[Girardet *et al.*, 2014] B. Girardet, L. Lapasset, D. Delahaye, and C. Rabut. Wind-optimal path planning: Application to aircraft trajectories. In *Proc. of ICARCV*, pages 1403–1408, 2014.

[Isern-Gonzalez *et al.*, 2011] J. Isern-Gonzalez, D. Hernandez-Sosa, E. Fernandez-Perdomo, J. Cabrera-Gamez, A. C. Domnguez-Brito, and V. Prieto-Maranon. Path planning for underwater gliders using iterative optimization. In *Proc. of IEEE ICRA*, pages 1538–1543, 2011.

[Janson *et al.*, 2015] L. Janson, E. Schmerling, A. Clark, and M. Pavone. Fast Marching Tree: A fast marching sampling-based method for optimal motion planning in many dimensions. *Int. J. Rob. Res.*, 34(7):883–921, 2015.

[Jones *et al.*, 2014] C. Jones, B. Allsup, and C. DeCollibus. Slocum glider: Expanding our understanding of the oceans. In *Proc. of IEEE OCEANS*, pages 1–10, 2014.

[Ko *et al.*, 2014] I. Ko, B. Kim, and F. C. Park. Randomized path planning on vector fields. *Int. J. Rob. Res.*, 33(13):1664–1682, 2014.

[Kularatne *et al.*, 2016] D. Kularatne, S. Bhattacharya, and M. A. Hsieh. Time and Energy Optimal Path

Planning in General Flows. In *Proc. of RSS*, pages 47–57, 2016.

[Lawrance and Sukkarieh, 2011] N. Lawrance and S. Sukkarieh. Autonomous exploration of a wind field with a gliding aircraft. *J. Guid. Control Dynam.*, 34(3):719–733, 2011.

[Leonard and Graver, 2001] N. Leonard and J. Graver. Model-based feedback control of autonomous underwater gliders. *IEEE J. Ocean. Eng.*, 24(4):633–645, 2001.

[Liu *et al.*, 2017] Y. Liu, J. Ma, N. Ma, and G. Zhang. Path planning for underwater glider under control constraint. *Adv. Mech. Eng.*, 9(8):1–9, 2017.

[Lolla *et al.*, 2014a] T. Lolla, P. J. Haley Jr., and P. F. J. Lermusiaux. Time-optimal path planning in dynamic flows using level set equations: realistic applications. *Ocean Dyn.*, 64(10):1399–1417, 2014.

[Lolla *et al.*, 2014b] T. Lolla, P. F. J. Lermusiaux, M. P. Ueckermann, and P. J. Haley Jr. Time-optimal path planning in dynamic flows using level set equations: theory and schemes. *Ocean Dyn.*, 64(10):1373–1397, 2014.

[M. *et al.*, 2015] S. M., D. M., and A. K. W. C. Trajectory optimization of an autonomous dynamic soaring UAV. In *Proc. of ICCC*, pages 95–100, 2015.

[Mahmoudian *et al.*, 2010] N. Mahmoudian, J. Geisbert, and C. Woolsey. Approximate analytical turning conditions for underwater gliders: Implications for motion control and path planning. *IEEE J. Ocean. Eng.*, 35(1):131–142, 2010.

[Nguyen *et al.*, 2013] J. Nguyen, N. Lawrance, R. Fitch, and S. Sukkarieh. Energy-constrained motion planning for information gathering with autonomous aerial soaring. In *Proc. of IEEE ICRA*, pages 3825–3831, 2013.

[Rao and Williams, 2009] D. Rao and S. B. Williams. Large-scale path planning for Underwater Gliders in ocean current. In *Proc. of ARAA ACRA*, 2009.

[Şucan *et al.*, 2012] I. A. Şucan, M. Moll, and L. E. Kavraki. The Open Motion Planning Library. *IEEE Rob. Autom. Mag.*, 19(4):72–82, December 2012. `http://ompl.kavrakilab.org`.

[Tesei *et al.*, 2015] A. Tesei, R. Been, D. Williams, B. Cardeira, D. Galletti, D. Cecchi, B. Garau, and A. Maguer. Passive acoustic surveillance of surface vessels using tridimensional array on an underwater glider. In *Proc. of IEEE OCEANS*, pages 1–8, 2015.

[Witt and Dunbabin, 2014] J. Witt and M. Dunbabin. Go with the flow: Optimal AUV path planning in coastal environments. In *Proc. of ARAA ACRA*, 2014.

[Xinke *et al.*, 2015] Z. Xinke, J. Xianglong, Y. Jiancheng, and L. Yiping. Path planning in stronger ocean current for underwater glider. In *Proc. of IEEE CYBER*, pages 891–895, 2015.

[Yoo *et al.*, 2012] C. Yoo, R. Fitch, and S. Sukkarieh. Probabilistic temporal logic for motion planning with resource threshold constraints. In *Proc. of RSS*, 2012.

[Yoo *et al.*, 2014] C. Yoo, R. Fitch, and S. Sukkarieh. Online task planning and control for aerial robots with fuel constraints in winds. In *Proc. of WAFR*, 2014.

[Zarafshan *et al.*, 2008] P. Zarafshan, S. B. Moosavian, S. A. A. Moosavian, and M. Bahrami. Optimal control of an Aerial Robot. In *Proc. of IEEE/ASME AIM*, pages 1284–1289, 2008.

[Zermelo, 1931] E. Zermelo. *ber das Navigationsproblem bei ruhender oder vernderlicher Windverteilung*, volume 11. WILEY-VCH Verlag, 1931.

A Variables in trim state

For a trim state $\tau_k = [V_k, \gamma_k, \delta_k, m_{bk}]^T$, the trim variables are described as follows

$$\begin{aligned} V_k^d &= \sqrt{\frac{m_b^d - (m - m_h - \bar{m})}{-\sin\gamma_k^d(K_{D_0} + K_D{\alpha_k^d}^2) + \cos\gamma_k^d(K_{L_0} + K_L\alpha_k^d)}} \\ \gamma_k^d &= \alpha_k^d + \theta_k^d \\ m_{bk}^d &= \begin{cases} m_{b\max} & \text{if } z_f > 0 \\ 0 & \text{otherwise} \end{cases}, \end{aligned} \tag{14}$$

where

$$\begin{aligned} \alpha_k^d &= \frac{K_L}{2K_D}\tan\gamma_k^d \\ &\quad \left(-1 + \sqrt{1 - \frac{4K_D}{{K_L}^2}\cot\gamma_k^d(K_{D_0}\cot\gamma_k^d + K_{L_0})}\right) \\ x_p &= -z_{P_d}\tan\theta_d \\ &\quad + \frac{\left((m_{f3} - m_{f1})\,u_d w_d + \left(K_{M_0} + K_M\alpha^d\right)V^{d2}\right)}{\bar{m}g\cos\theta_d}. \end{aligned}$$

The heading angle δ_k^d is calculated by substituting the the above variables to the x- or y-term in (9). Note that we only consider x_p where y_p and z_p are fixed parameters.

B Glider parameters

Parameter	Value
J_2	0.1 Nm^2
m	11.22 kg
$\bar{m}$	2.0 kg
$m_{b\max}$	2.0 kg
m_h	8.22 kg
m_{f1}	2.0 kg
m_{f3}	14.0 kg
K_{D_0}	5 $N(s/m)^2$
K_D	20 $N(s/m)^2$
K_{L_0}	0 $N(s/m)^2$
K_L	306 $N(s/m)^2$
K_{M_0}	0 $Nm(s/m)^2$
K_M	-36.5 $Nm(s/m)^2$
L_H	1 (J/s)